Journal of Nanotechnology and Innovative Materials

Review Article

Structural phase transitions and control of superionic transport in copper and silver chalcogenides

Yusif. I. Aliyev[1,2], Ophelya. R. Babayeva[1], and Sevinc. R. Azimova[3]

[1]Azerbaijan State Pedagogical University, Baku, Azerbaijan
[2]Western Caspian University, 31 Istiglaliyyat Street, Baku, Azerbaijan.
[3]Institute of Physics, Ministry of Science and Education of the Republic of Azerbaijan, Baku, Azerbaijan

Received: 27.07.2026 Accepted: 26.09.2026 Published: 12.10.2026
https://doi.org/10.54414/BJSA1833

Copyright: © 2026 by the authors. Licensee: Journal of Nanotechnology and Innovative Materials, Western Caspian University, Baku, Azerbaijan. This article is an open-access article distributed under the terms and conditions of the Creative Commons Attribution 4.0 International License (CC BY 4.0).

Abstract

Chalcogenides of copper and silver have been proposed as prospective thermoelectrics due to their low thermal conductivity, strong anharmonicity, polymorphism with temperature dependence, and liquid-like mobility of the cation in the high-temperature phases. The current review analyzes published data concerning high-temperature X-ray diffraction, differential thermal analysis, and ab initio investigations of Cu2Se, Ag2S, AgCuS, AgCuSe, Cu4Se1.5Te0.5, and Cu4Te1.5Se0.5 in a unified comparative way. Three key factors determining their functional behavior are outlined: disordering of the Cu+/Ag+ sublattice within a relatively intact anion framework; transitions from lower-symmetry structures to higher-symmetry cubic modifications; and the impact of substitutions of cations and anions on transition temperatures and properties of the carrier–phonon interaction. Characteristic temperatures are given as 407 K for the orthorhombic-cubic transition in Cu2Se, about 450 K for the acanthite-argentite transition in Ag2S, and 930 K for the Cmcm-Fm$\bar{3}$m transition in AgCuS. The phenomena of structural transformations and thermal events in the Cu–Se–Te materials cover a wider temperature regime and need to be interpreted on a case-by-case basis. Thermodynamics and kinetics of the phenomenological framework link free energy, ion site occupation, correlation of diffusion, and transport. This framework has not been parameterized based on data obtained for specific materials and does not provide new experimental or ab initio information. Structure mapping, concurrent analysis of the structure and calorimetry, transport properties study, and operando mobility studies have been suggested for phase control and stability assessment.

Keywords: copper and silver chalcogenides; superionic conduction; structural phase transitions; cation disorder; thermoelectric materials; solid solutions; high-temperature X-ray diffraction; phase stability

1. Introduction

Conversion of thermal energy into electrical energy without any mechanical energy is the physical principle on which thermoelectric generators work. They operate without noise, have no moving parts, and can be designed for particular purposes. Performance of materials is measured in terms of the dimensionless parameter $zT=S^2\sigma T/\kappa$, where S is the Seebeck coefficient, σ is the electrical conductivity, T is the absolute temperature, and κ is the total thermal conductivity. The interrelation between these properties makes it hard to decrease thermal conductivity without decreasing electrical conductivity. Copper and silver chalcogenides have a unique property that is determined by their crystal structure: while a rigid anion sublattice serves as the periodic medium for the electron flow, mobile cations in the high-temperature phase serve as the medium for phonon scattering [1], [2], [3], [4].

Cu2Se is a prototypical example of a phonon-liquid/electron-crystal system. Recent works have considered the significant variation of electrical and thermal transport properties near the phase transition of this compound, along with high zT values and the issues associated with cation movement and device reliability [3], [4], [5], [6]. The Ag2S and Ag2Se systems are of special importance for low-temperature thermoelectric

applications and flexible and wearable devices [7], [8], [9], [10]. Ternary compounds such as AgCuS and AgCuSe can be considered model systems for understanding the competition between the two cations in their site preference for the same anion framework. Cu-Se-Te solid solutions can be used to study the impact of anion size and bond polarizability on phase stability [11], [12], [13], [14], [15], [16].

Nonetheless, such materials are frequently considered as distinct classes of materials. This review attempts to consolidate the previous studies conducted by the author and other recent studies in order to reveal common structural motifs and to develop a general phase engineering approach to functional chalcogenides. Special emphasis is placed on the differences between structural transitions, predicted ion dynamics, and observed transport phenomena.

2. Materials and methods

The present research is a structured comparative analysis of already existing scientific results and not experimental work. The data set includes high-temperature X-ray diffraction (XRD) investigation of Cu2Se in the range 290 – 1000 K [11] XRD and differential thermal analysis (DTA) of AgCuS [12], Density functional theory (DFT) study of the electronic structures of Ag2S and Ag2Se [13], reversible dissociation and combination reaction in the Ag-Cu-Se system [14], polymorphism in AgCuSe0.5(S,Te)0.5 compounds [15] and DTA and XRD of Cu4Se1.5Te0.5 and Cu4Te1.5Se0.5 systems [16], [17]. The general structural information is provided by the comparative study on cation and anion substitution in the chalcogenides [18]. The sequence of XRD for the tellurium-rich composition is additionally presented in a public dissertation abstract [19].

Four parameters are used in this comparison: room-temperature symmetry and phase composition; typical transformation temperature; high-temperature symmetry and reversibility; and potential transport properties implications. Obtained temperatures from different techniques cannot be considered equal to one another. XRD identifies crystal structure change while DTA observes heat effect. Kinetics, heating rate, sample treatment, volatiles, and nonstoichiometry could result in discrepancies between the temperatures presented. This problem is especially critical when comparing XRD transformation at 558 K and DTA transformation around 800 K in Cu4Se1.5Te0.5 [16], [17]. Synthesis is literature- and source-based. It is not a review or meta-analysis.

3. Results and discussion

3.1. Cu_2Se from low symmetry to a superionic cubic phase

The temperature-driven transformation of Cu2Se is used as the reference for comparison. In the corresponding author's X-ray diffraction study performed at high temperatures, it was suggested that the room-temperature crystal structure corresponds to the orthorhombic form of the substance with the space group $P222_1$, and a transition to a cubic form with the space group $F\bar{4}3m$ occurs at 407 K [11]. The transition temperature is in agreement with other published data that fall within the range of 400-414 K [3], [4], [5], [6]. In the course of the transition, the selenium lattice remains intact, while copper cations populate a variety of sites.

A combination of higher symmetry on an average crystalline scale and dynamic disorder at the local scale is a hallmark of superionic thermoelectrics. A decreased phonon mean free path can lower κL even when the concentration and mobility of carriers are still strongly dependent on copper vacancies. Nonetheless, high zT in and of itself does not guarantee technological stability. Copper migration, compositional modifications at electrode boundaries, and oxidation may constrain long-term stability when the material is operated under electrical current and a temperature gradient [5], [6].

3.2. Ag_2S and AgCuS in two cation mobility regimes

At low temperatures, Ag2S is a semiconductor that crystallizes with the acanthite structure (monoclinic system) and has a space group of $P2_1/c$. At a temperature above about 450 K, Ag2S crystallizes in the higher symmetry argentite structure and shows superionic conductivity [7], [8], [20]. The first-principles calculations by the corresponding author have shown that Ag2S with a monoclinic structure ($P2_1/c$) is a semiconductor, while its higher symmetry could make it semimetallic [13]

For AgCuS, the conversion of the orthorhombic Cmcm structure at room temperature to the cubic $Fm\bar{3}m$ structure at 930 K is marked by a DTA endotherm with a peak at 938 K [12]. It can be seen from its higher transition temperature compared to Ag2S that it has a different enthalpy and entropy relationship; however, it cannot show whether the migration energy is higher than that of Ag2S.

3.3. AgCuSe and mixed cation systems

AgCuSe is both a distinct ternary compound and an important intermediate phase in the Ag–Cu–Se phase equilibria. The high-temperature face-centered cubic (fcc) modification of $Ag_{1.5}Cu_{0.5}Se$ reversibly decomposes into Ag_2Se + AgCuSe below 488 K, whereas $Ag_{0.4}Cu_{1.6}Se$ reversibly decomposes into Cu_2Se + AgCuSe below 540 K [14]. These observations identify AgCuSe as a chemical bridge between silver-rich and copper-rich compositions.

3.4. Phase boundary control by anion substitution in Cu–Se–Te

Substitution of tellurium for selenium leads to the alteration of anion mass, ionic radius, bond polarizability, and lattice anharmonicity. According to the high-temperature XRD analysis, the low-temperature $R\bar{3}m$ phase of Cu4Se1.5Te0.5 exhibits a reversible transformation into the cubic phase with the lattice constant a ~ 5.899 Å [17] at 558 K. Endothermic effects appear at 413 and 800 K, while the exothermic effect is detected at 725 K for Cu4Se1.5Te0.5, and endothermic effects are registered at 410, 465, and 800 K for Cu4Te1.5Se0.5 [16]. Signals around 410 and 465 K could relate to adsorbed water or surface phenomena. The issue of whether the effect at 800 K is associated with a phase transition, structural rearrangement, or other processes is to be solved via a joint XRD-DSC-TGA analysis. The published dissertation abstract states that decomposition of Cu4Te1.5Se0.5 occurs at ~ 770 K into the hexagonal Cu2(SeTe)0.5 and cubic Cu2Te phases, and the cubic phase appears at 850 K [19].

The discrepancy between the XRD and DTA temperatures is supposed to be investigated as a possible sign of a multistage process instead of a contradiction. One possible scenario is that local or partial structural rearrangement begins at lower temperature, whereas a bulk transformation or a thermally more pronounced event occurs at higher temperature. Testing this hypothesis requires simultaneous high-temperature XRD–DSC, temperature-dependent Raman spectroscopy, and electrical and thermal transport measurements on the same sample.

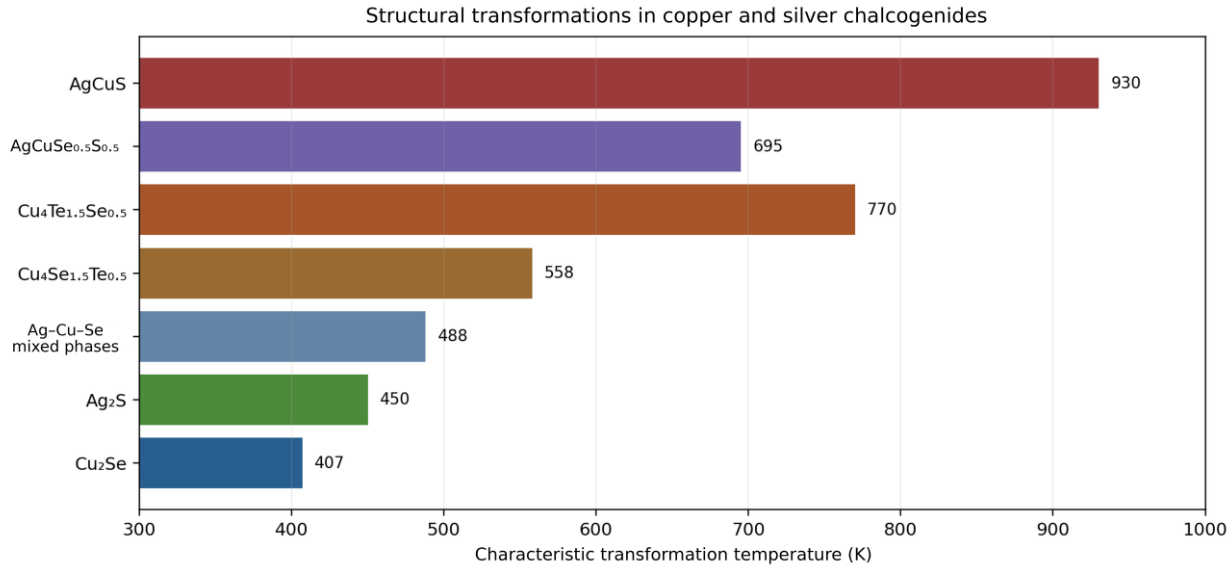


Figure 1. Comparison of characteristic structural transformation temperatures in copper and silver chalcogenides based on published data. For Ag–Cu–Se, 488 K denotes the reversible boundary $Ag_{1.5}Cu_{0.5}Se \rightleftharpoons Ag_2Se$ + AgCuSe; for $Cu_4Te_{1.5}Se_{0.5}$, 770 K denotes the onset of phase separation observed by high-temperature XRD. DTA peak temperatures and XRD phase boundaries are methodologically distinct and should not be treated as the same physical quantity [11], [12], [13], [14], [15], [16], [17], [19], [20].

3.5. A theoretical framework for phase stability, cation dynamics, and transport

The following phenomenological framework is proposed for the systems compared here. Composition, temperature, and defects alter phase free energies, cation site occupancies, and hopping kinetics, which influence electronic and thermal transport through distinct channels. High average symmetry can coexist with dynamic disorder, but the observation of a cubic phase by XRD does not by itself prove superionic conduction. The framework presents no new DFT, ab initio molecular dynamics (AIMD), or experimental results. Its purpose is to connect published observations with testable thermodynamic and kinetic relationships.

3.5.1. Free energy and disordering

At constant pressure and fixed overall composition, the free-energy difference between the high-temperature phase H and the low-temperature phase L is written as

$$\Delta G(T,x) = G_H - G_L = \Delta H(T,x) - T\Delta S(T,x) \quad (1)$$

Here, x is the substitution fraction, and ΔH and ΔS are the enthalpy and entropy differences expressed using the same molar normalization. At an equilibrium boundary, ΔG = 0. For a first-order transition, if ΔH and ΔS are approximately constant near the transition, $T_t \approx \Delta H/\Delta S$; this relation does not automatically apply to a continuous transition. Entropy includes configurational, vibrational, and electronic contributions. Differences between heating and cooling boundaries can reflect nucleation and kinetic delay in addition to the equilibrium transition temperature.

$$S_{conf} = -R \Sigma_s \nu_s \Sigma_i y_{is} \ln y_{is}, \quad \Sigma_i y_{is} = 1$$

In this expression, νs represents the number of sites of kind s per mole of formula units, while yis represents the fraction of occupancy of component i on those sites, vacancies being considered a different kind of component whenever needed. The above expression is based on independent and ideally mixed sites, without considering short-range interactions. The entropy resulting from the mixing of Cu and Ag and the entropy resulting from the redistribution of cations on further sites cannot be counted twice as the same effect. (2)

3.5.2. Mixing and phase separation

$$\Delta G_{mix} = \Omega x(1-x) + RT[x \ln x + (1-x)\ln(1-x)] \quad (3)$$

Ω is the molar interaction parameter in the symmetric binary regular solution approximation. The stability of a homogeneous system is assured only if $\partial^2G/\partial x^2 > 0$; negative $\partial^2G/\partial x^2$ suggests spinodal decomposition instability. Two-phase equilibrium occurs by the common tangent method. At a constant, positive Ω, the theory predicts a critical temperature of Tc = Ω/(2R). Figure 2b conceptually illustrates the preference for a two-phase state at low temperature and the dominance of mixing entropy at higher temperature. Real Ag–Cu–Se and Cu–Se–Te systems are multicomponent. Calculating their phase boundaries requires a separate Gibbs-energy description for each phase, stoichiometric constraints, and mass balance. Since Ω is not fitted here, the model does not yield new material-specific phase-boundary temperatures.

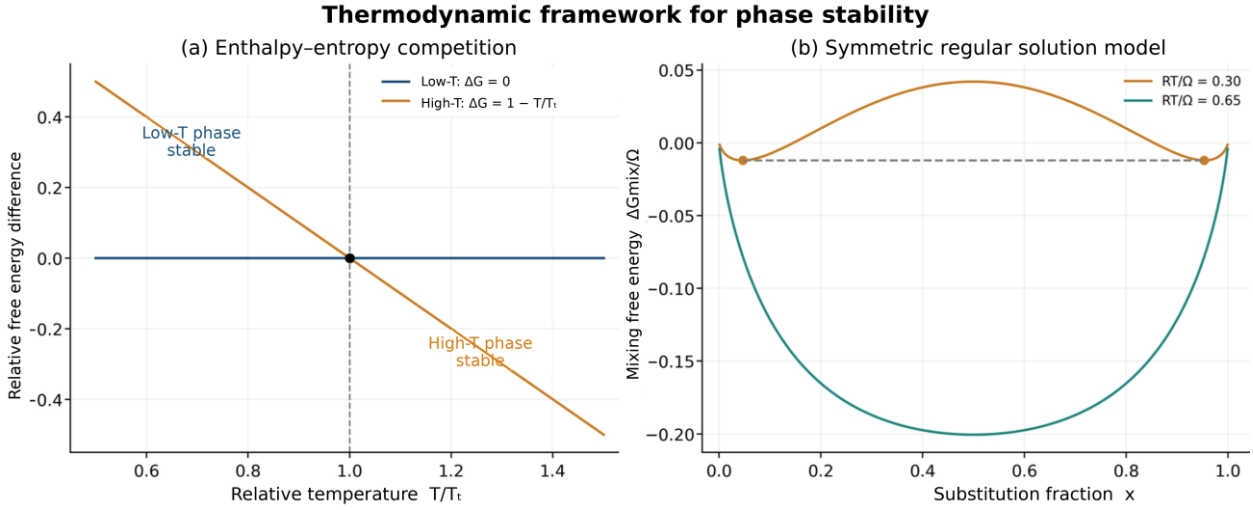


Figure 2. Conceptual thermodynamic framework. (a) $\Delta G/\Delta H = 1 - T/T_t$ for constant ΔH and ΔS, with the low-temperature phase used as the reference. (b) Dimensionless mixing-free-energy curves, $\Delta G_{mix}/\Omega$, for a symmetric regular solution with $\Omega > 0$; the dashed line is the common tangent to the low-temperature curve. The dimensionless parameters are illustrative and are not fitted to experimental data.

3.5.3. Diffusion and mixed conduction

$$D^*(T) = D_0 \exp[-\frac{E_a}{k_B T}], \quad \sigma_{ion} = \frac{n_i q_i^2 D_\sigma}{k_B T} \tag{4}$$

D* is the tracer self-diffusion coefficient, D_0 is the pre-exponential factor, E_a is the effective activation energy, n_i is the volumetric concentration of mobile ions, q_i is the ionic charge, and D_σ is the conductivity diffusion coefficient. The values of D* and Dσ can be considered equal only under uncorrelated conditions; correlations are measured using the Haven ratio HR = D*/Dσ. When the concentration of vacancies is a function of temperature, then Ea can be different from the activation energy of a single jump.

Arrhenius fitting should be restricted to a single phase and comparable defect regimes.

$$\sigma_{tot} = \sigma_{el} + \sigma_{ion}, \quad t_{ion} = \frac{\sigma_{ion}}{\sigma_{tot}} \tag{5}$$

The above decomposition relies on a linear response of a homogeneous material subjected to suitable boundary conditions. In the case of ion-blocking electrodes, the long-time direct current response will differ from the transient and alternating current response. Therefore, it becomes imperative that the conductivities be separated using impedance techniques, selection of suitable electrodes, and polarization studies. The flux of ions depends on the concentration gradient, electric field, and temperature gradient. DFT calculations with the NEB approach and AIMD calculations are two such complementary methods.

3.5.4. Phonon and electronic transport

$$\kappa = \kappa_L + \kappa_{el}, \quad \kappa_L \approx \frac{C_V v_s \ell}{3}, \quad \kappa_{el} \approx L\sigma_{el}T \tag{6}$$

The heat capacity per unit volume is denoted by CV, the characteristic sound velocity is vs, and the phonon mean free path is ℓ. The kinetic relation holds true only as long as the quasiparticle theory for phonons is applicable; its applicability in the strongly anharmonic superionic state needs to be determined independently. The Wiedemann–Franz separation demands that the appropriate value for L be selected, taking into account the nature of the band structure and the scattering regime. Equation (6) will have to be modified in case of bipolar or other transport processes. The variations in mass, strain, interface effects, and anharmonicity affect κL [1], [2]. Nonetheless, neutron scattering data for Cu2Se do not justify the hypothesis that ion hopping destroys transverse phonons completely. [21].

$$\sigma_{el} \approx ne\mu, \quad zT_{el} = \frac{{S_{el}}^2 \sigma_{el} T}{\kappa_L + \kappa_{el}}$$

Under a single dominant carrier assumption, n is the carrier density, μ is carrier mobility, and e is the elementary charge. Sel represents the Seebeck coefficient at the steady state. Structural fluctuations may change band edges and the carrier-phonon interaction [4]. Nevertheless, information on Sel, σel, and κ must be measured under identical temperature and phase conditions. The presence of heat-capacity anomalies, latent heat, and transient temperature fields near a phase transition point may impact measurements. The direct substitution of measured total electrical conductivity and transient thermoelectric voltage into Equation (7) thus needs to be justified for the mixed conductor. Figure 3 summarizes independent approaches to verify the approach. (7)

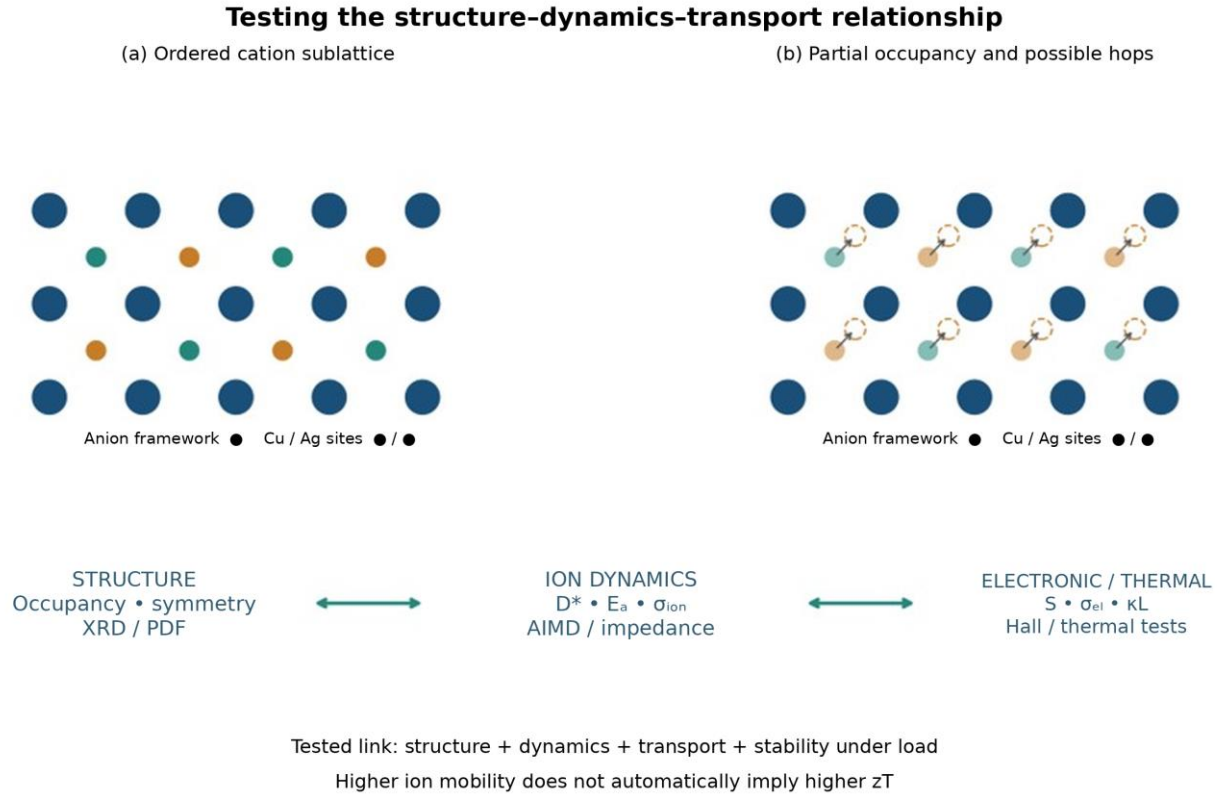


Figure 3. Conceptual diagram of the structure–dynamics–transport relationship. Blue circles denote the anion framework, orange and green circles denote cation sites, and dashed outlines indicate alternative sites. Arrows represent possible hops. The geometry does not depict the unit cell, site occupancies, or migration pathways of a specific compound. PDF denotes the atomic pair distribution function. The lower part shows the combined validation of structural, dynamic, and functional measurements.

3.5.5. Testable predictions and limitations

First, if the entropy advantage of the high-temperature phase is a principal driving force, changes in site occupancies should be consistent in direction with the calorimetric entropy change. Such agreement is not conclusive because vibrational contributions are also present. Second, if Cu↔Ag substitution restricts ion motion, D* or σ_{ion} should decrease, or the fitted E_a should increase, at the same temperature and in comparable phase and defect states. The opposite outcome would not support the migration-restriction hypothesis.

Third, if a secondary phase enhances phonon scattering, κ_L should decrease after accounting for density and electronic heat transport. A proposed energy-filtering effect requires that an increase in S_{el} cannot be explained solely by a change in carrier concentration and must be supported by interfacial-barrier and mobility data. Fourth, if the events at 558 and 800 K belong to a single multistage process, the temperature evolution of phase fractions should correlate with thermal effects in the same sample. Mass loss or the appearance of new phases would require alternative explanations.

These available data do not allow for dependable quantification of values of ΔH, ΔS, Ω, Ea, D0, or HR. The model does not offer, thus, a fitting predictive calculation. The significance of the proposed model lies in establishing connections between structural features and certain measurable parameters of thermodynamic stability and conductivity.

Table 1. Comparative summary of structural transformations in copper and silver chalcogenides.

System	Low-temperature state	Characteristic T (K)	High-temperature outcome	Functional implications
Cu_2Se	Orthorhombic $P222_1$	407	Cubic $F\bar{4}3m$	Superionic Cu sublattice; low κ_L; stability assessment required
Ag_2S	Monoclinic $P2_1/c$	≈450	Cubic argentite	Ductility and near-room-temperature thermoelectric relevance
AgCuS	Orthorhombic Cmcm	930 (XRD); 938 (DTA)	Cubic $Fm\bar{3}m$	Collective cation disorder at high temperature
Ag–Cu–Se	Multiphase	488–540	fcc composition field	Phase and interface engineering through intermediate AgCuSe
$AgCuSe_{0.5}S_{0.5}$	$Cu_{1.96}S$ + AgCuSe	695	Single fcc phase	Phase-boundary tuning by anion substitution
$Cu_4Se_{1.5}Te_{0.5}$	$R\bar{3}m$	558 (XRD); 800 (DTA)	Cubic phase / thermal event	Possible multistage transformation
$Cu_4Te_{1.5}Se_{0.5}$ [22]	Trigonal/multiphase	770–850 (XRD)	Phase separation → cubic phase	More complex kinetics in the Te-rich composition

Note: XRD phase boundaries, decomposition onsets, and DTA peak temperatures describe different observables. fcc denotes face-centered cubic.

4. Future research directions

What follows will be the determination of the time-, composition-, and load-dependent behavior of the transformation phenomena rather than the identification of additional isolated transition temperatures. The primary concern should be the joint analysis of XRD-DSC and transport properties on the same material at high temperature. It would prove whether there is any coincidence in the timing for the beginning of structural change, thermal effects, and anomalous Seebeck or conductivity response. Special attention should be paid to the transient behavior of the Seebeck coefficient [4].

The second objective will be to develop a composition-temperature-phase map for cation substitution in Cu ↔ Ag along with anion substitution in S ↔ Se ↔ Te. The goal here would be to ensure that the transition takes place slightly below the required operating window, with a single phase maintaining symmetry being used throughout operation and minimal decomposition taking place with thermal cycling. The third objective will be testing of the operando stability by measuring the migration of Cu/Ag cations near electrodes in a temperature gradient and with DC current using scanning electron microscopy with EDS or WDS, micro-XRD, and impedance spectroscopy.

Hypothesis: Suitable amounts of mixed cations and mixed anions could inhibit phononic energy transfer due to mass fluctuation and strain effects. Coherent or nanoscale AgCuSe-like phases could act as energy filters; the presence of silver ions could limit the diffusion of copper. The above-mentioned benefits can be considered useful in technological applications only when stability and durability under electrical loading are proven.

5. Conclusion

The main takeaway is that both the structural, thermal, and electronic aspects of the phase transitions need to be measured simultaneously, instead of relying on an isolated value of zT to evaluate performance. For the

optimization of this material class, there must be a compromise between nearness to the phase transition point and stability during operation. Such a comparison can be carried out rationally using simultaneous measurement of XRD-DSC-transport, composition analysis, and migration studies under operando conditions. This is made possible by the thermodynamic and kinetic framework that we have outlined. The figures shown are not new experimental or first-principles calculations.

The key finding is the importance of studying the structural, thermal, and electronic contributions to phase transitions in tandem, rather than assuming high zT implies good performance. Optimizing this class of materials entails the delicate balancing act of being near a phase boundary while also being operationally stable. A combination of XRD-DSC-transport measurements, compositional analysis, and operando ion migration studies forms the rationale behind the proposed approach for assessing tunable superionic chalcogenides. The suggested thermodynamic and kinetic model allows this to be evaluated via quantitative metrics on free energy, site occupancy, ion diffusion, and electron transport. The example figures shown here are not new data or first-principles results.

Acknowledgments
The authors thank Dr. Sakin Jabarov (Doctor of Sciences in Physics) for his assistance in preparing this manuscript.

Funding information
This research did not receive any specific grant from funding agencies in the public, commercial, or not-for-profit sectors.

Conflict of interest statement
The authors declare no conflicts of interest.

Data availability
This review uses previously published findings identified in the reference list. No new experimental dataset is reported. Figures 2 and 3 are conceptual illustrations, and their parameters are not fitted to experimental data.

References

[1] Liu H, Shi X, Xu F, Zhang L, Zhang W, Chen L, Li Q, Uher C, Day T, Snyder GJ. Copper ion liquid like thermoelectrics. Nature materials. 2012 May;11(5):422-5. https://doi.org/10.1038/nmat3273

[2] He J, Tritt TM. Advances in thermoelectric materials research: Looking back and moving forward. Science. 2017 Sep 29;357(6358):eaak9997. https://doi.org/10.1126/science.aak9997

[3] K, Choi S, Hirata K, Adachi M, Kiyama M, Matsuura T, Yamamoto Y, Matsunami M, Takeuchi T. Discovery of colossal Seebeck effect in metallic Cu2Se. Nature communications. 2019 Jan 8;10(1):72. https://doi.org/10.1038/s41467-018-07877-5

[4] Zhao K, Yue Z, Wuliji H, Chen H, Deng T, Lei J, Qiu P, Chen L, Shi X. Modeling critical thermoelectric transports driven by band broadening and phonon softening. Nature Communications. 2024 Jan 26;15(1):776. https://doi.org/10.1038/s41467-024-45093-6

[5] Ying P, Jian Q, Gong Y, Song T, Yang Y, Geng Y, Huang J, Sun R, Chen C, Shen T, Li Y. Matrix plainification leads to high thermoelectric performance in plastic Cu2Se/SnSe composites. Nature Communications. 2025 Apr 7;16(1):3305. https://doi.org/10.1038/s41467-025-58484-0

[6] Nieroda P, Rudnik M, Mitoraj-Królikowska M, Drożdż E, Kozień D, Leszczyński J, Koleżyński A. Investigating the Stability of Cu2Se Superionic Thermoelectric Material in Air Atmosphere. Materials. 2025 Sep 4;18(17):4152. https://doi.org/10.3390/ma18174152

[7] Zhou WX, Wu D, Xie G, Chen KQ, Zhang G. α-Ag2S: A ductile thermoelectric material with high ZT. ACS omega. 2020 Mar 10;5(11):5796. https://doi.org/10.1021/acsomega.9b03929

[8] [Simonnin P, Sassi M, Gilbert B, Charlet L, Rosso KM. Phase transition and liquid-like superionic conduction in Ag2S. The Journal of Physical Chemistry C. 2020 Apr 14;124(18):10150-8. https://doi.org/10.1021/acs.jpcc.0c00260
[9] Zhu M, Shi XL, Wu H, Liu Q, Chen ZG. Advances in Ag2S-based thermoelectrics for wearable electronics: progress and perspective. Chemical Engineering Journal. 2023 Oct 1;473:145236. https://doi.org/10.1016/j.cej.2023.146194
[10] Lyu JM, Zhang L, Yang YL, Zhu JF, Shi XL, Chen ZG. Ag2Se-Based thermoelectric materials and devices: progress, challenges, and perspectives. Energy & Environmental Science. 2026 May 26;19(10):3134-83. https://doi.org/10.1039/D6EE01371F
[11] Dashdemirov AO, Aliyev YI, Bashirov RJ, Aliyeva NA, Rustamova LV. Structural aspects of the thermal properties of the Cu2Se. International Journal of Modern Physics B. 2024 Apr 20;38(10):2450150. https://doi.org/10.1142/S0217979224501509
[12] Aliyev YI, Asadov YG, Ilyasli TM, Mammadov FM, Naghiyev TG, Ismayilova ZA, Mirzayev MN, Jabarov SH. Structural aspects of thermal properties of AgCuS compound. Modern Physics Letters B. 2020 Feb 20;34(05):2050066. https://doi.org/10.1142/S0217984920500669
[13] Aliyev YI, Ismayilova NA, Novruzov RF, Dashdamirov AO, Huseynov HJ, Jabarov SH, Ayubov AA. Electron structure and density of states' calculations of Ag2S and Ag2Se crystals from first-principle. Modern Physics Letters B. 2019 Jul 30;33(21):1950242. https://doi.org/10.1142/S0217984919502427
[14] Aliyev YI, Asadov YG, Dashdemirov AO, Aliyeva RD, Naghiyev TG, Jabarov SH. Polymorphic transformations and thermal expansion of some modifications in Ag 1. 5 Cu 0. 5 Se and Ag 0. 4 Cu 1. 6 Se. International Journal of Modern Physics B. 2019 Sep 20;33(23):1950271. https://doi.org/10.1142/S0217979219502710
[15] Aliyev YI, Asadov YG, Aliyeva RD, Jabarov SH. Polymorphic transformations and thermal expansion in AgCuSe0. 5 (S, Te) 0.5 crystals. Semiconductors. 2017 Jun;51(6):732-9. https://doi.org/10.1134/s1063782617060045
[16] Aliyeva NA, Aliyev YI, Abiyev AS. Study of thermal properties of Cu4Se1. 5Te0. 5 and Cu4Te1. 5Se0. 5 compounds by differential thermal analysis. Advanced Physical Research. 2022;4(2):94-9. https://jomardpublishing.com/UploadFiles/Files/journals/APR/V4N2/Aliyeva_et_al.pdf
[17] Gasimova NA, Amiraslanov IR, Aliyev YI, Guseinov GG. Structure and Phase Transitions of Cu 4 Se 1.5 Te 0.5. InAIP Conference Proceedings 2011 Dec 26 (Vol. 1400, No. 1, pp. 476-479). American Institute of Physics. https://doi.org/10.1063/1.3663166
[18] Asadov YG, Aliyev YI, Babaev AG. Polymorphic transformations in Cu2Se, Ag2Se, AgCuSe and the role of partial cation-cation and anion-anion replacement in stabilizing their modifications. Physics of Particles and Nuclei. 2015 May;46(3):452-74. https://doi.org/10.1134/s106377961503003x
[19] Əliyeva NA. $Cu_4X_{2-m}Y_m$ tərkibli birləşmə və bərk məhlulların kristal quruluşu və quruluş faza keçidləri (X, Y = S, Se, Te; m = 0.0; 0.25; 0.50; 0.75) [fəlsəfə doktoru dissertasiyasının avtoreferatı]. 2021. https://aak.gov.az/upload/dissertasion/fizika/avtoreferat_ing_.pdf
[20] Sadovnikov SI, Kostenko MG, Gusev AI, Lukoyanov AV. Low-temperature predicted structures of Ag2S (Silver Sulfide). Nanomaterials. 2023 Sep 25;13(19):2638. https://doi.org/10.3390/nano13192638
[21] Voneshen DJ, Walker HC, Refson K, Goff JP. Hopping time scales and the phonon-liquid electron-crystal picture in thermoelectric copper selenide. Physical review letters. 2017 Apr 7;118(14):145901. https://doi.org/10.1103/physrevlett.118.145901